Proceeding of the IEEE
International Conference on Robotics and Biomimetics
Dali, China, December 2019

Design and Optimization of Single-degree-of-freedom Six-bar Mechanisms for Knee Joint of Lower Extremity Exoskeleton Robot*

1st Bo Xiao and 3rd Yixin Shao

School of Mechanical Engineering and Automation

Beihang University
Beijing, China

{xiaobo & shaoyx2014}@buaa.edu.cn

2nd Wuxiang Zhang*

School of Mechanical Engineering and Automation, Beijing
Advanced Innovation Center for Biomedical Engineering
Beihang University
Beijing, China

zhangwuxiang@buaa.edu.cn

***Abstract* - The irregular contact surface between the femur and the tibia of the human body produces J-shaped instantaneous centers of rotation (ICR) of the knee joint. Therefore, two single-degree-of-freedom (SDOF) six-bar mechanisms, which are composed of a trajectory fitting four-bar mechanism and a transmission four-bar mechanism, are used to fit the centers of the human knee joint and increase the load-bearing performance. Firstly, the displacements of ICR of the human knee joint are measured and calculated for the sake of the dimensional synthesis of the trajectory fitting four-bar mechanism. Then, two structural layouts of transmission four-bar mechanism are designed according to different selection of the driving rod in the trajectory fitting four-bar mechanism, and both the transmission four-bar mechanisms are optimized. The results show that after the two-step optimization, the SDOF six-bar mechanism with the crank as the driving rod in the trajectory fitting four-bar mechanism has a better performance in smoothing the knee joint torque curve and superior transmission efficiency.**

Index Terms* - *exoskeleton, knee joint, instantaneous center of rotation, dimensional synthesis.

I. Introduction

The lower extremity exoskeleton robot is a wearable human-machine integrated intelligent equipment. The equipment provides weight-bearing support and motion enhancement for the wearer to reduce physical exertion and risk of physical damage under the complex terrain environment. Nowadays, the lower extremity exoskeleton robot has become the hotspot in the field of robotics.

As the important transmission mechanism between the exoskeleton hip joint and the ankle joint, the knee joint needs to bear a huge amount of weight. In order to improve the load bearing performance and stability of exoskeleton robots, a lot of relevant studies were conducted around the world. In terms of structure, the four-bar mechanism is often used in exoskeletons and prostheses because of its simple structure and better performance in fitting the instantaneous centers of rotation (ICR) of the human knee joint [1]. For instance, Singh [2] proposed the TLBO algorithm to simplify the dimensional synthesis of the four-bar mechanism. Hyun [3] added a rolling bearing into the four-bar mechanism to improve the bearing performance of the knee joint. In other aspects, Sun [4] added a pair of gears into the five-bar mechanism to enhance its performance in fitting the ICR of the knee joint. Choo [5] applied a linear actuator and a sub-link mechanism to the knee joint, greatly increasing the payload capacity of the exoskeleton. Chen [6] used the linear series elastic actuator (SEA) to increase the ability of the exoskeleton to withstand impact. However, the studies above either only focus on the transmission mechanism or only focus on the fitting mechanism. Thus, based on the ICR of the human knee joint, two single-degree-of-freedom (SDOF) six-bar mechanisms with different configurations are used for trajectory fitting and torque transmission in the study, and their transmission performance is obtained.

The outline of the paper is as follows. In Section 2, the displacements of the ICR of the human knee joint are measured and calculated. Section 3 presents the dimensional synthesis of the trajectory fitting four-bar mechanism and the transmission four-bar mechanisms. Section 4 compares and analyzes the transmission ratio and driving angle of these two SDOF six-bar mechanisms. Conclusions are drawn in Section 5.

II. Measurement And Calculation

The human knee joint consists of the lower end of the femur, the upper end of the tibia and the patella. Due to the irregular contact surface between the femur and the tibia, the instantaneous central axis of the knee joint is not fixed. Studies have shown that the ICR of the knee joint is roughly a J-shaped curve when the knee is bending [7]. In order to improve the comfort for the wearer and the stability for the exoskeleton, the knee joints are always designed into multi-axis mechanisms, fitting the J-shaped ICR.

A healthy adult male with a height of 1750 mm was selected as the experimental subject. To mitigate the effect of the thigh muscles and the calf muscles, two bamboo boards each with four markers were attached to the outside of the thigh and calf. Before the experiment, the male subject sat in the center of the acquisition space of the motion capture system, facing the positive *x*-axis of the world coordinate system, and the plane of the bamboo boards should be roughly parallel to the *xoz* plane of the world coordinate system. As the experiment began, the male subject swung the calf freely in the *xoz* plane at

* Supported by National Key R&D Program of China (Grant No. 2016YFE0105000) and National Natural Science Foundation of China (Grant No. 91848104).

978-1-7281-6321-5/19//$31.00 ©2019 IEEE

a constant velocity while the motion capture system recorded the coordinate changes of the eight markers at a sampling frequency of 100 Hz. The acquisition lasted for 20 seconds and 6 sets of cycle data were obtained. The experimental process is shown in Fig. 1.

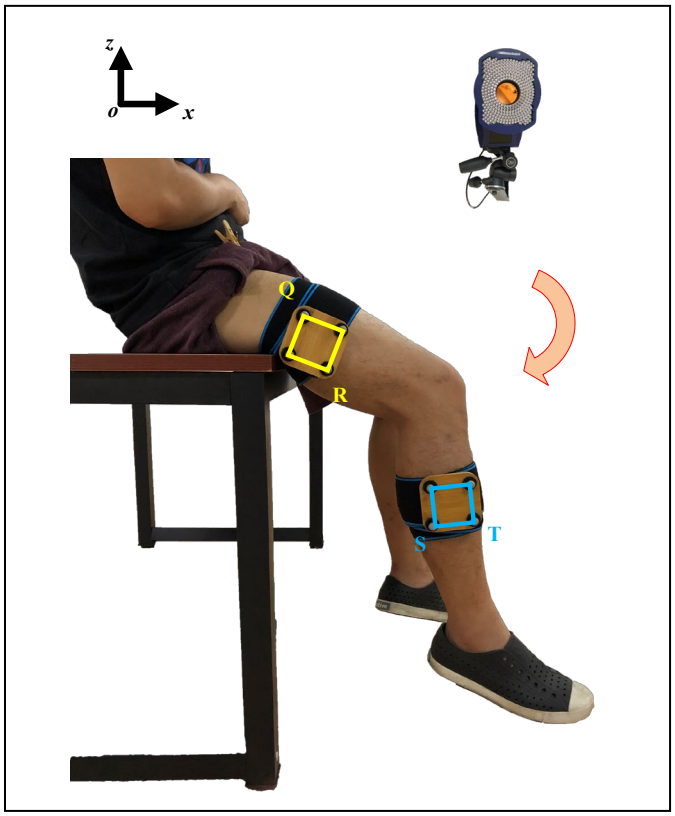

Fig. 1 The experimental process

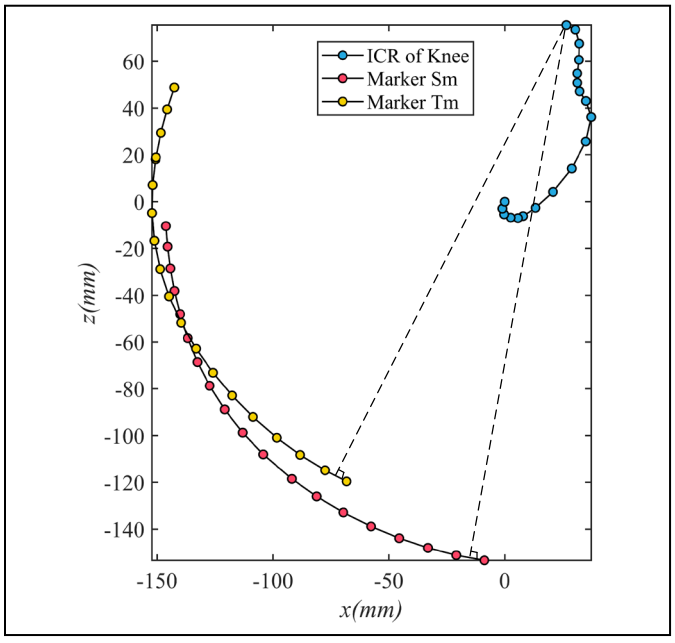

Fig. 2 The ICR of the knee joint

TABLE I
THE COORDINATES OF THE ICR

Knee Flexion Angle (°)	*x* (mm)	*z* (mm)	Knee Flexion Angle (°)	*x* (mm)	*z* (mm)
10	26.6	75.5	60	28.9	14.1
15	30.5	73.6	65	20.9	4.2
20	32.2	67.6	70	13.3	-2.6
25	32	60.6	75	7.9	-6.2
30	31.3	54.8	80	5.7	-7
35	31.4	50.8	85	2.6	-6.8
40	32.3	47.1	90	-0.3	-5.4
45	35.1	43	95	-1	-2.9
50	37.3	36.2	100	0	0
55	35	25.7			

Due to the difference in angular velocity of each cycle, the smoothest set of data is selected for further analysis. Firstly, two markers are randomly selected separately from the thigh and the calf, and their connections are recorded as *QR* and *ST*. Then, fixing the line *QR* on the thigh in the world coordinate system and correcting the position of *ST* with the slight displacement generated by *QR* in the subsequent movement. After the correction, marker S_m and marker T_m are obtained, showing in Fig. 2. Finally, backtracking the ICR of the knee joint in the sagittal plane with the modified marker S_m and marker T_m. A set of ICR of the knee joint (converted to standing state) are obtained and shown in Table I and Fig. 2. From Fig. 2, it can be easily observed that ICR of the knee joint is a J-shaped curve, ranging from -7 to 75.5 along the *z*-axis and ranging from -1 to 35.1 along the *x*-axis.

III. DIMENSIONAL SYNTHESIS

A. Dimensional Synthesis for the Trajectory Fitting Four-bar Mechanism

The four-bar mechanism is one of the most commonly used and most mature mechanisms for multi-axis artificial knee joints because of its great performance in fitting ICR of the human knee joint and its simple structure [1]. There are also many commercially available prosthetic products based on the four-bar mechanism. In this study, the four-bar mechanism will be optimized to fit the ICR of the human knee joint. The optimization method is the function fmincon which is good at solving the minimum value of the nonlinear multivariate functions in MATLAB; the optimization target is to fit the ICR of the human knee joint as much as possible; the optimization constraints include the existence of a double crank mechanism and transmission angle constraints; the parameters of four-bar mechanism include the structural angle α and the lengths of the links l_i (i = 1,2,3,4). The designed ICR and the optimal dimensional parameters are shown in Fig. 3 and Table II, respectively.

B. Two Structural Layouts of the Transmission Four-bar Mechanism

Thanks to the dimensional synthesis for trajectory fitting four-bar mechanism, the exoskeleton knee joint can well fit the

J-shaped ICR of the human knee joint [8]. Next, two structural layouts of transmission four-bar mechanism are proposed, namely direct drive mode and distal drive mode. In the direct drive mode, the link *AB* is the actuating part, directly driven by the motor. Such a driving mode removes the intermediate transmission mechanism and improves the transmission efficiency and mechanism stability. However, because the motor and sensors are placed at the end of the thigh, the increased rotational inertia of the thigh rod makes it a little more difficult for the precise control of the exoskeleton and increases the torque requirement of the hip joint. In the distal drive mode, the motor is placed at the upper middle of the thigh, and the lower leg is driven through a transmission mechanism. Although this driving mode adds the transmission mechanism, it could reduce rotational inertia of the exoskeleton lower limbs. Finally, the distal drive mode is selected, and another four-bar mechanism is used as the transmission mechanism. Two structural layouts of transmission four-bar mechanism are designed according to different selection of the driving rod in the trajectory fitting four-bar mechanism. These two mechanisms are respectively named as the connecting-rod-drive transmission four-bar mechanism and the crank-drive transmission four-bar mechanism. Their sketches are shown in Fig. 5.

C. Dimensional Synthesis for the Transmission Four-bar Mechanisms

The goal of dimensional synthesis for transmission four-bar mechanism is to improve the transmission performance of the mechanism. As for the human knee joint, there are always one or two peaks with huge amplitude in the torque curve during the motion cycle, making it a little more difficult for motor control. By analyzing the human clinical gait analysis (CGA) data [9], the absolute values of the maximum joint torque of the human body at different knee flexion angles (the knee flexion angle range of human body when climbing is between 10° and 94°) are counted, as shown in Fig.4, for dimensional synthesis of transmission four-bar mechanism.

1) Connecting-rod-drive Transmission Four-bar Mechanism (Stephenson III):

a) Inverse Kinematic Analysis

The coordinate system and geometric parameters of the connecting-rod-drive transmission four-bar mechanism are defined in the left side of Fig. 5. As shown in Fig. 5, the geometric parameters include the structural angles α, β and the lengths of links l_i (i = 1,2, ···,8). The component OAF is fixed as the frame while link EF is the actuating part (the distance from F to OA along the z-axis is set to l_F). In addition, based on the optimization results of the trajectory fitting four-bar mechanism, instantaneous center $P(x_P, z_P)$ and $B(x_B, z_B)$ can be obtained with different angle θ_3 (θ_3 is the knee flexion angle ranging from -10° to -94°). The angle θ_5 can be obtained via inverse kinematics.

The closed-loop vector equation is:

$$\overrightarrow{OF} + \overrightarrow{FE} + \overrightarrow{ED} = \overrightarrow{OB} + \overrightarrow{BD} \tag{1}$$

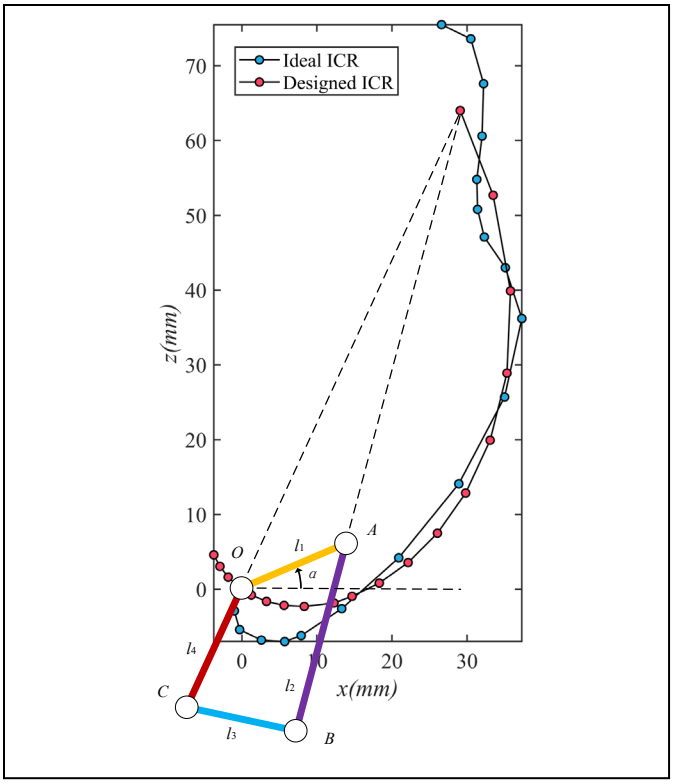

Fig. 3 Comparison between the ideal ICR and designed ICR

TABLE II
THE OPTIMAL DIMENSIONAL PARAMETERS OF FOUR-BAR MECHANISM

Parameters	l_1 (mm)	l_2 (mm)	l_3 (mm)	l_4 (mm)	α (rad)
Optimal results	30	80	55	65	0.35

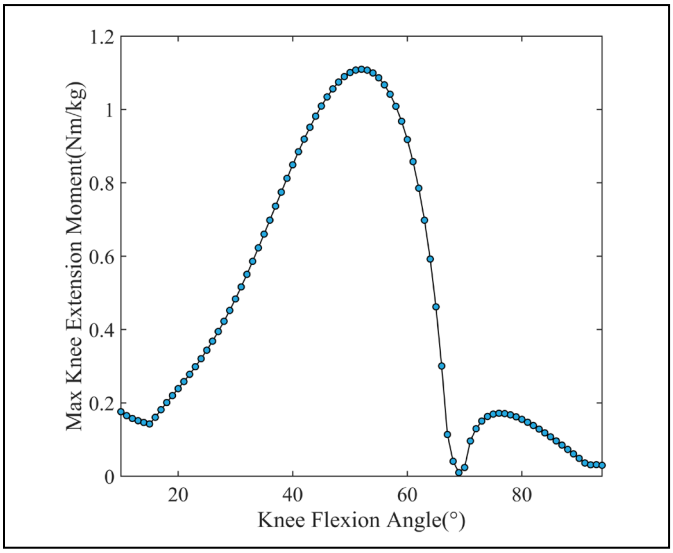

Fig. 4 The maximum torque at different knee flexion angles

which can be described as:

$$\begin{cases} a + l_5 \cos\theta_5 + l_6 \cos\theta_6 = c \\ b + l_5 \sin\theta_5 + l_6 \sin\theta_6 = d \end{cases} \tag{2}$$

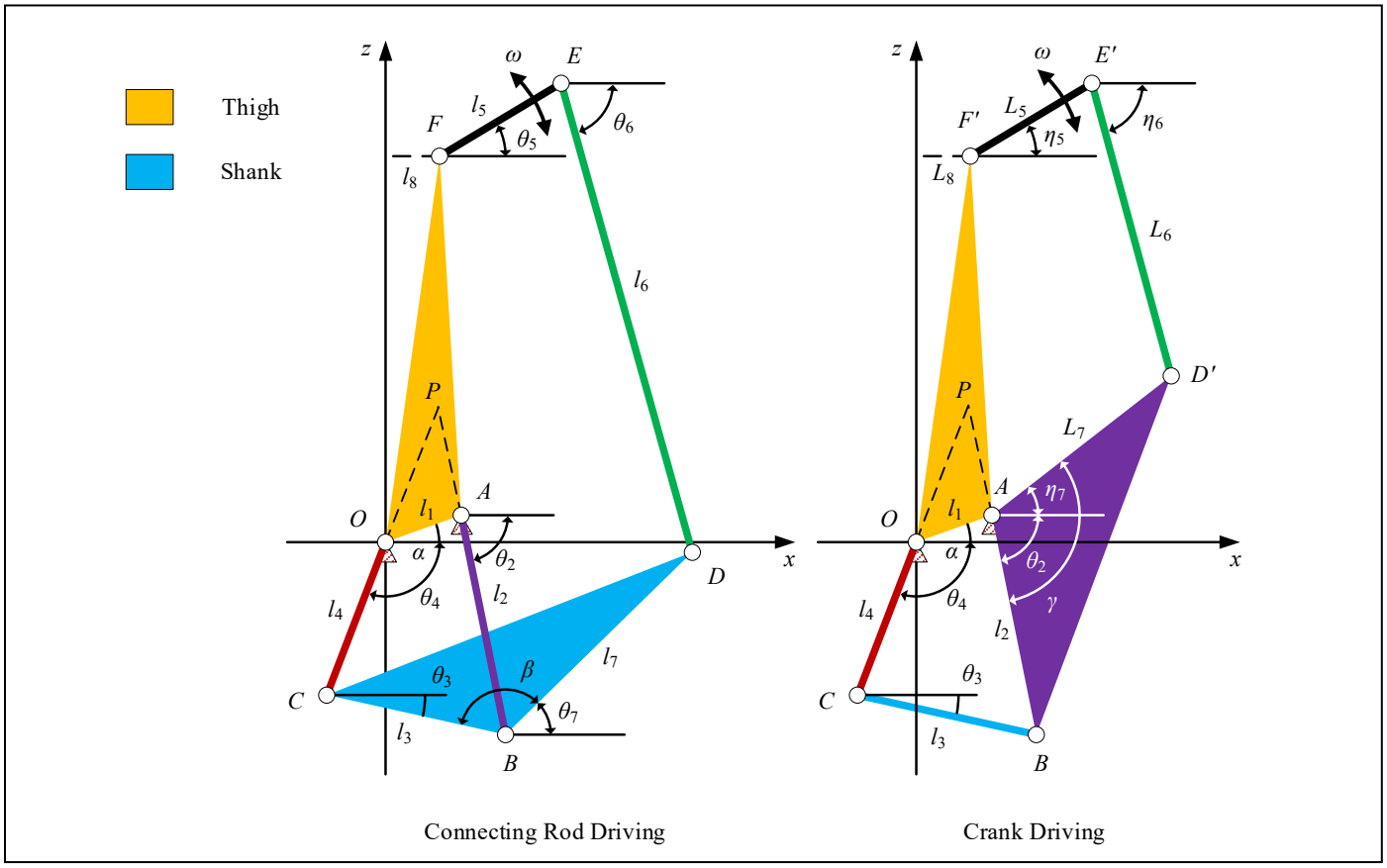

Fig. 5 Sketches of the connecting-rod-drive transmission four-bar mechanism and the crank-drive transmission four-bar mechanism

where $a = l_8, b = l_F + l_8 \tan\alpha, c = x_B + l_7 \cos\theta_7$, $d = z_B + l_7 \sin\theta_7$, $\theta_7 = \pi + \theta_3 - \beta$

The trigonometric equation can be obtained from (2):

$$A_1 \cos\theta_5 + B_1 \sin\theta_5 = C_1 \tag{3}$$

where $A_1 = 2l_5(c-a)$, $B_1 = 2l_5(d-b)$, $C_1 = (c-a)^2 + (d-b)^2 + {l_5}^2 - {l_6}^2$

The angle θ_5 can be solved as:

$$\sin\theta_5 = \frac{2B_1C_1 \pm \sqrt{(2B_1C_1)^2 - 4({A_1}^2+{B_1}^2)({C_1}^2-{A_1}^2)}}{2({A_1}^2+{B_1}^2)} \tag{4}$$

Point $E(x_E, z_E)$ and point $D(x_D, z_D)$ can be obtained using (4), then equation of the line ED can be described as:

$$A_2x + B_2z + C_2 = 0 \tag{5}$$

where $A_2 = z_D - z_E$, $B_2 = x_E - x_D$, $C_2 = (x_D - x_E)z_E - (z_D - z_E)x_E$

The vertical distance from point F to line ED and from point P to line ED is:

$$l_{F-ED} = \left| \frac{A_2x_F + B_2z_F + C_2}{\sqrt{{A_2}^2+{B_2}^2}} \right|$$

$$l_{P-ED} = \left| \frac{A_2x_P + B_2z_P + C_2}{\sqrt{{A_2}^2+{B_2}^2}} \right|$$

The transmission ratio of the connecting-rod-drive transmission four-bar mechanism can be obtained:

$$i_1 = \frac{l_{P-ED}}{l_{F-ED}} \tag{6}$$

b) Constraints

According to the Grashof criterion, constraints of the rods lengths are as follows:

$$\begin{cases} g_1(X_1) = l_5 + l_6 - l_{FP} - l_{DP} \le 0 \\ g_2(X_1) = l_5 - l_6 + l_{FP} - l_{DP} \le 0 \\ g_3(X_1) = l_5 - l_6 - l_{FP} + l_{DP} \le 0 \end{cases} \tag{7}$$

where l_{FP} and l_{DP} are the lengths of FP and DP, $X_1 = \{l_5, l_6, l_7, l_8, \beta\}$ is the design parameters vector for the connecting-rod-drive transmission four-bar mechanism

The transmission angle of the mechanism when the human knee joint torque is maximum is set to 60° or more:

$$g_4(X_1) = \frac{x_{DE}x_{DP}+z_{DE}z_{DP}}{\sqrt{x_{DE}{}^2+z_{DE}{}^2}\sqrt{x_{DP}{}^2+z_{DP}{}^2}} - \cos\frac{\pi}{3} \le 0 \qquad (8)$$

where x_{DE} and x_{DP} are the lengths of DE and DP along the x-axis, z_{DE} and z_{DP} are the lengths of DE and DP along the z-axis

c) Goal Function

The required torque output by the motor is determined by $\tau(\theta_3)$, the absolute values of the maximum joint torque of the human body at different knee flexion angles. So the goal function is to minimize the required torque output by the motor.

$$\max\left[\frac{\tau(\theta_3)}{i_1}\right] + \sum_{j=1}^{4}(\max(0, g_j))^2 \rightarrow \min \qquad (9)$$

In order to solve the optimization synthesis problem, the function fmincon in MATLAB is employed. The boundaries of the design parameters and the optimal dimensional parameters are shown in Table III.

2) Crank-drive Transmission Four-bar Mechanism (Watt-II):

The coordinate system and geometric parameters of the crank-drive transmission four-bar mechanism are defined in the right side of Fig. 5. As shown in Fig. 5, the geometric parameters include the structural angles α, γ and the lengths of links l_i (i = 1,2,3,4), L_i (i = 5,6,7,8). The component OAF' is fixed as the frame while link $E'F'$ is the actuating part (the distance from F' to OA along the z-axis is set to $l_{F'}$). In addition, based on the optimization result of the trajectory fitting four-bar mechanism, instantaneous center $P(x_P, z_P)$ and $B(x_B, z_B)$ can be obtained with different angle θ_3 (θ_3 is the knee flexion angle ranging from -10° to -94°). The angle η_5 can be obtained via inverse kinematics. Using a similar processing method as in the previous section, the goal function of the crank-drive transmission four-bar mechanism can be obtained:

$$\max\left[\frac{\tau(\theta_3)}{i_2}\right] + \sum_{j=1}^{4}(\max(0, G_j))^2 \rightarrow \min \qquad (10)$$

where i_2 is the transmission ratio and G_j are the constraints

To solve the optimization synthesis problem, the function fmincon in MATLAB is employed. The boundaries of the design parameters and the optimal dimensional parameters are shown in Table IV.

TABLE III
THE BOUNDARIES AND OPTIMAL RESULTS OF STEPHENSON III MECHANISM

Parameters	l_5 (mm)	l_6 (mm)	l_7 (mm)	l_8 (mm)	β(rad)
Lower boundary	60	200	100	0	2π/3
Upper boundary	100	300	200	30	π
Optimal results	93	224	145	29	2.2

TABLE IV
THE BOUNDARIES AND OPTIMAL RESULTS OF WATT-II MECHANISM

Parameters	L_5(mm)	L_6(mm)	L_7(mm)	L_8(mm)	γ(rad)
Lower boundary	60	150	50	0	2π/3
Upper boundary	100	250	100	30	π
Optimal results	69	187	80	21	2.3

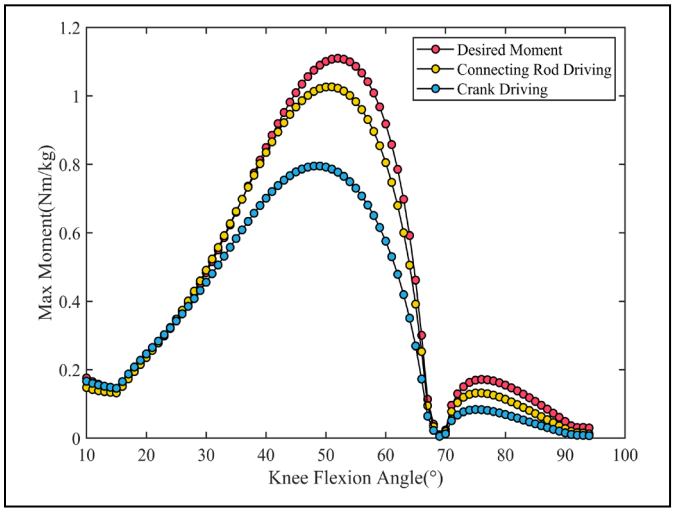

Fig. 6 Comparison of the required toque output by motor between the two SDOF six-bar mechanisms

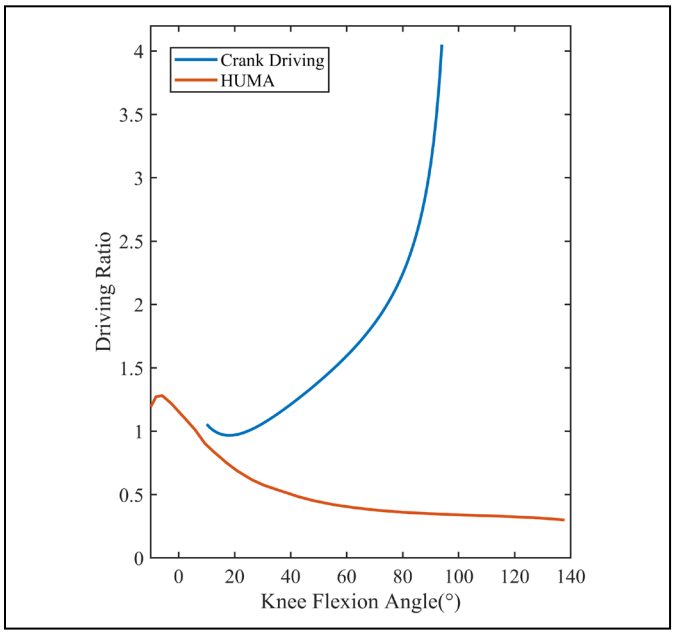

Fig. 7 Comparison of the driving ratio between HUMA and the optimized crank-drive transmission four-bar mechanism

IV. ANALYSIS AND DISCUSSION

As we can see from the human CGA data, there are always one or two peaks with huge amplitude in the torque curve during knee joint movement [9], making it a little more difficult for motor control. Therefore, the kinematics analysis of the

connecting-rod-drive transmission four-bar mechanism and the crank-drive transmission four-bar mechanism are implemented respectively, and the optimized torque curves of these two SDOF six-bar mechanisms are obtained, as shown in Fig. 6. From Fig. 6, both mechanisms have positive effect on the knee joint torque curve, especially at the knee angle of 40° to 60°. However, the crank-drive transmission four-bar mechanism performs better with the drop of 0.3423 Nm/kg at the peak torque, which shows that the crank-drive transmission four-bar mechanism has a better smoothing effect on the knee joint torque curve. On the other hand, the HUMA exoskeleton [3] designed by Hyun adopted a similar mechanism configuration of knee joint as the crank-drive transmission four-bar mechanism, and the comparison of the driving ratio between HUMA and the optimized crank-drive transmission four-bar mechanism is shown in Fig. 7. From Fig. 7, the driving ratio of HUMA is always below 1.0, which indicates its motor has to input more torque to satisfy the output torque. However, after optimization, the crank-drive transmission four-bar mechanism is required to input much less torque.

The transmission angle is an important performance indicator of the mechanism. So, the transmission angle at the knee flexion angle with the maximum knee torque is also used as the constraint in the dimensional synthesis of the transmission four-bar mechanisms. For deeper understanding of the overall transmission performance of the two mechanisms during the movement, all the transmission angles are recorded, as shown in Fig. 8. The transmission angle of the crank-drive transmission four-bar mechanism is always greater than 55° during the knee flexion while the transmission angle of the connecting-rod-drive transmission four-bar mechanism drops below 50° when the knee flexion angle reaches 78°. As reaching to the extreme angle of the knee flexion, the transmission angle of the connecting-rod-drive transmission four-bar mechanism drops down to 30°, which is very detrimental for torque to transfer. The results show that the crank-drive transmission four-bar mechanism has an advantage in transmission efficiency.

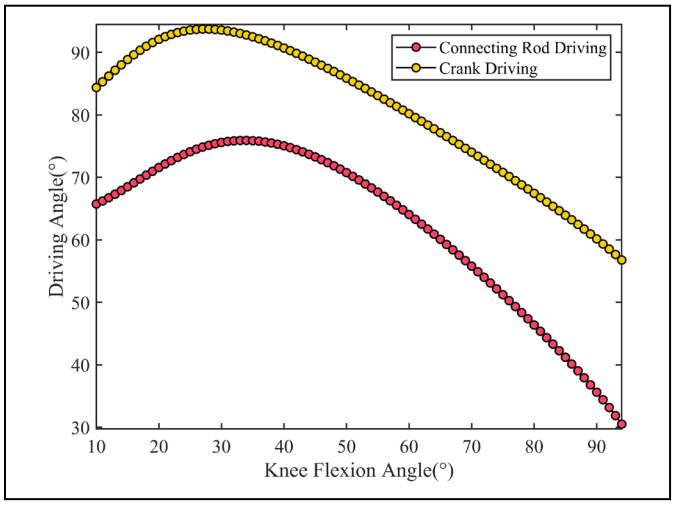

Fig. 8 Comparison of the transmission angles between the two SDOF six-bar mechanisms

V. Conclusions

The ICR of the human knee joint are measured and calculated for the dimensional synthesis of the trajectory fitting four-bar mechanism. In order to eliminate the influence of leg muscle on the measurement result, two bamboo boards are used in the experiment to ensure that all markers are roughly on the same plane. After correcting the coordinates of markers on the calf, a set of well-fit ICR of the knee joint is obtained.

The fmincon method in MATLAB is used for the dimensional synthesis of the trajectory fitting four-bar mechanism. Two structural layouts of transmission four-bar mechanism are designed according to different selection of the driving rod in the trajectory fitting four-bar mechanism. The optimal dimensional parameters of these two SDOF six-bar mechanisms are obtained, with the knee joint torque in the CGA data as input, with the transmission angle as the constraints and with the required minimum torque output by the motor as the goal function.

By analyzing the transmission ratio and transmission angle of these two SDOF six-bar mechanisms, the transmission performance of the two mechanisms during knee flexion is obtained. The results show that the SDOF six-bar mechanism with the crank as the driving rod in the trajectory fitting four-bar mechanism has a better performance in smoothing the knee joint torque curve and superior transmission efficiency.

References

[1] J. W. Breakey and S. H. Marquette, "Beyond the Four-Bar Knee," *Jpo Journal of Prosthetics & Orthotics*, vol. 10, no. 3, 1998.

[2] R. Singh, H. Chaudhary, and A. K. Singh, "Defect-free optimal synthesis of crank-rocker linkage using nature-inspired optimization algorithms," *Mechanism and Machine Theory*, vol. 116, pp. 105-122, Oct 2017.

[3] D. J. Hyun, H. Park, T. Ha, S. Park, and K. Jung, "Biomechanical design of an agile, electricity-powered lower-limb exoskeleton for weight-bearing assistance," *Robotics and Autonomous Systems*, vol. 95, pp. 181-195, Sep 2017.

[4] Y. Sun, W. Ge, J. Zheng, and D. Dong, "Design and evaluation of a prosthetic knee joint using the geared five-bar mechanism," *IEEE Trans Neural Syst Rehabil Eng*, vol. 23, no. 6, pp. 1031-1038, Nov 2015.

[5] J. Choo and J. H. Park, "Increasing payload capacity of wearable robots using linear actuators," *IEEE-ASME Transactions on Mechatronics*, vol. 22, no. 4, pp. 1663-1673, Aug 2017.

[6] G. Chen, P. Qi, Z. Guo, and H. Y. Yu, "Mechanical design and evaluation of a compact portable knee-ankle-foot robot for gait rehabilitation," *Mechanism and Machine Theory*, vol. 103, pp. 51-64, Sep 2016.

[7] E. Piña-Martínez and E. Rodriguez-Leal, "Inverse modeling of human knee joint based on geometry and vision systems for exoskeleton applications," *Mathematical Problems in Engineering*, vol. 2015, pp. 1-14, 2015.

[8] D. A. Hobson and L. E. Torfason, "Optimization of four-bar knee mechanisms—A computerized approach," *Journal of Biomechanics*, vol. 7, no. 4, pp. 371-376, Jan 1974.

[9] A. Protopapadaki, W. I. Drechsler, M. C. Cramp, F. J. Coutts, and O. M. Scott, "Hip, knee, ankle kinematics and kinetics during stair ascent and descent in healthy young individuals," *Clinical Biomechanics*, vol. 22, no. 2, pp. 203-210, Feb 2007.